Synthesis of *O*-(3-[^{18}F]Fluoropropyl)-L-tyrosine (L-[^{18}F]FPT) and Its Biological Evaluation in 9L Tumor Bearing Rat†

Byung Seok Moon, Sang Wook Kim, Tae Sup Lee, Soon Hyuk Ahn, Kyo Chul Lee, Gwang Il An, Seung Dae Yang, DaeYoon Chi,‡ Chang Woon Choi,# Sang Moo Lim,# and Kwon Soo Chun*

Laboratory of Cyclotron Application, Korea Institute of Radiological and Medical Sciences, Seoul 139-706, Korea
**E-mail: kschun@kcch.re.kr*
‡Department of Chemistry, Inha University, Incheon 402-751, Korea
#Department of Nuclear Medicine, Korea Institute of Radiological and Medical Sciences, Seoul 139-706, Korea
Received September 10, 2004

O-(3-[^{18}F]Fluoropropyl)-L-tyrosine (L-[^{18}F]FPT) was synthesized by nucleophilic radiofluorination followed by acidic hydrolysis of protective groups and evaluated with 9 L tumor bearing rat. L-[^{18}F]FPT is an homologue of *O*-(2-[^{18}F]fluoroethyl)-L-tyrosine (L-[^{18}F]FET) which recently is studied as a tracer for tumor imaging using positron emission tomography (PET). [^{18}F]FPT was directly prepared from the precursor of *O*-(3-*p*-toluenesulfonyloxypropyl)-*N*-(*tert*-butoxycarbonyl)-L-tyrosine methyl ester. FPT-PET image was obtained at 60 min in 9 L tumor bearing rats. The radiochemical yield of [^{18}F]FPT was 40-45% (decay corrected) and the radiochemical purity was more than 95% after HPLC purification. The total time elapsed for the synthesis of [^{18}F]FPT was 100 min from EOB (End-of-bombardment). A comparison of uptake studies between [^{18}F]FPT and [^{18}F]FET was performed. In biodistribution, [^{18}F]FPT showed similar pattern with [^{18}F]FET in various tissues, but [^{18}F]FPT showed low uptake in brain. Furthermore, [^{18}F]FPT showed higher tumor-to-brain ratio than [^{18}F]FET. In conclusion, [^{18}F]FPT seems to be more useful amino acid tracer than [^{18}F]FET for brain tumors imaging with PET.

Key Words: *O*-(3-[^{18}F]Fluoropropyl)-L-tyrosine (L-[^{18}F]FPT), *O*-(2-[^{18}F]Fluoroethyl)-L-tyrosine (L-[^{18}F]FET), Tumor imaging, PET.

Introduction

Positron emitting radionuclide labeled amino acid analogs such as [^{18}F]fluorinated tyrosine derivatives recently have been proven to overcome the disadvantages of 2-[^{18}F]fluoro-2-deoxy-D-glucose ([^{18}F]FDG). [^{18}F]FDG is the most widely used radiotracer in tumor diagnosis using PET in clinic, but there have been some limitations that [^{18}F]FDG could not differentiate nonmalignant inflammatory tissue from tumor and showed lower contrast in brain tumor, to normal brain.[1,2] Although L-[^{11}C-methyl]methionine ([^{11}C]-MET) is a useful amino acid PET tracer for brain tumor imaging, its application is only limited to hospitals having own cyclotron due to short half-life of C-11.[3] Recent studies make much progress on simplified synthesis of L-[^{18}F]FET. L-[^{18}F]FET is known to be useful as an amino acid PET tracer for detection and localization of tumor with a high specificity than other available tracers.[4,5] Moreover, the uptake and image contrast of [^{18}F]FET appear to be very similar to those of [^{11}C]MET in PET studies of human brain tumours.[3] Although other fluorine-18 labeled amino acid derivatives such as fluorocyclobutane-1-carboxylic acid,[6] fluoroproline,[7] fluorophenylalanine,[8] tyrosine,[9,10] methyl tyrosine,[11,12] [^{18}F]FBPA (4-borono-2-[^{18}F]fluoro-L-phenylalanine),[13] and L-[^{18}F]FET have been reported, these materials have been shown low radiochemical and synthetic yields. Recently, L-[^{18}F]FPT, like other fluorinated analog of tyrosine, has been studied for tumor imaging but, low radiochemical yield has been reported and occasionally by-product could occur during reaction.[14-16] Recent systematic studies showed *in vitro* biological stability of fluoroalkyl groups, such as fluoromethyl, fluoroethyl, and fluoropropyl, using rat hepatic microsomes and human serum by Lee *et al.*[17] Although a couple of studies indicate [^{18}F]FPT is superior to FDG in the differentiation of tumor and inflammation and a potential amino acid tracer like [^{18}F]FET for tumor imaging, a direct comparison of [^{18}F]FET and [^{18}F]FPT has not been performed in brain tumor model.[14]

In this study, we developed novel method to promote the radiochemical yield with fluoropropyl tyrosine derivative from the mentioned results and evaluate the feasibility of [^{18}F]FPT as a new brain tumor imaging agent. Biological properties of [^{18}F]FPT were compared with those of [^{18}F]FET in 9L tumor bearing rat. Furthermore, PET imaging of [^{18}F]FPT was acquired in 9L tumor bearing rat.

Results and Discussion

Synthesis of *O*-(3-Fluoropropyl)-L-tyrosine (FPT). The precursor for direct [^{18}F]fluorination was synthesized from a commercially available material, *N*-(*tert*-butoxycarbonyl)-L-tyrosine methyl ester (**1**) as shown in Scheme 1. *O*-(3-*tert*-Butyldimethylsilyloxypropyl)-*N*-(*tert*-butoxycarbonyl)-L-

†Part of this work was presented at the 50th Annual Meeting of the Society of Nuclear Medicine, New Orleans, U.S.A., June 2003.

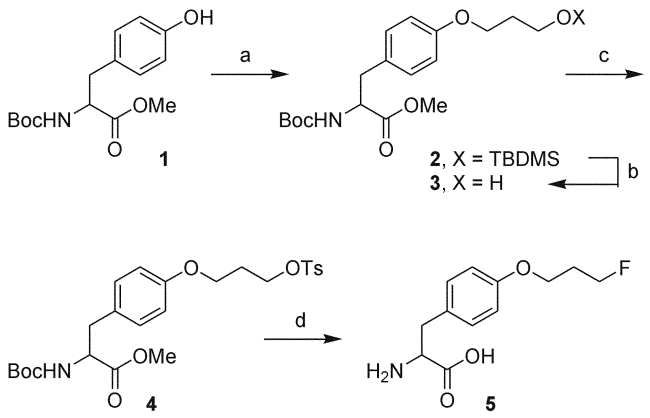

Scheme 1. Reaction conditions: a) (3-bromopropoxy)-*tert*-butyldimethylsilane, K_2CO_3, CH_3CN, rt, 3 days; b) $nBu_4NF \cdot 3H_2O$, THF, rt, 5 min; c) TsCl, TEA, CH_2Cl_2, rt, 3 h; d) $nBu_4NF \cdot 3H_2O$, CH_3CN, 90 °C, 20 min.

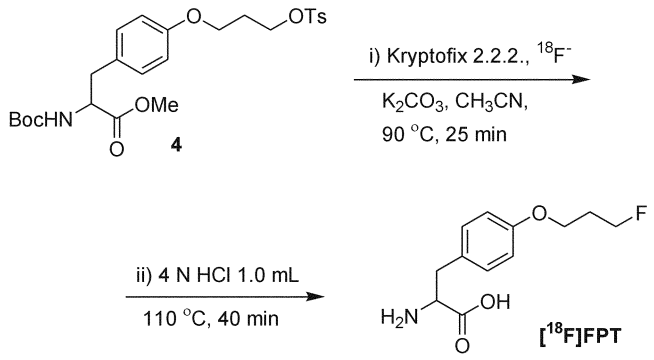

Scheme 2

tyrosine methyl ester was prepared by the reaction of *N*-(*tert*-butoxycarbonyl)-L-tyrosine methyl ester with 3-bromopropoxy-*tert*-butyldimethylsilane in yields of 70%, followed by deprotection of *tert*-butyldimethylsilane group using $nBu_4NF \cdot 3H_2O$ (TBAF·$3H_2O$). The precursor, tosylated compound, was prepared from *O*-(3-hydroxypropyl)-*N*-(*tert*-butoxycarbonyl)-L-tyrosine methyl ester with *p*-toluenesulfonyl chloride (*p*-TsCl) in the presence of triethylamine (TEA) in yields of 80%. The authentic FPT was synthesized from tosylated compound using TBAF·$3H_2O$ and 4 N HCl in yields of 44%.

The preparation of [^{18}F]FPT has been achieved by the nucleophilic substitution of precursor (**4**) with [^{18}F]fluoride ion in CH_3CN at 90 °C for 25 min followed by hydrolysis with 4 N HCl at 110 °C for 40 min as shown in Scheme 2. The isolation of the labeled compound was performed by HPLC using a semi-preparative column. The further purification was done by loading the purified [^{18}F]FPT through the strong cation exchange resin and collected pure [^{18}F]FPT with the phosphate buffered solution (pH = 7.4). The total time for the preparation of [^{18}F]FPT from EOB to EOS (End-of-synthesis) was 100 min. The quality control of the final product was conducted by HPLC using an analytical column.

Biodistribution of FET and FPT. The biodistribution data of [^{18}F]FPT and [^{18}F]FET in mice bearing 9L tumor are summarized in Table 1 and 2. The %ID/g in the blood of [^{18}F]FET injected mice decreased from 0.84 ± 0.07 at 10 min postinjection to 0.69 ± 0.06 at 120 min postinjection. The %ID/g in the blood of [^{18}F]FPT injected mice decreased from 0.97 ± 0.62 at 10 min postinjection to 0.52 ± 0.02 at 120 min postinjection. [^{18}F]FPT showed faster blood

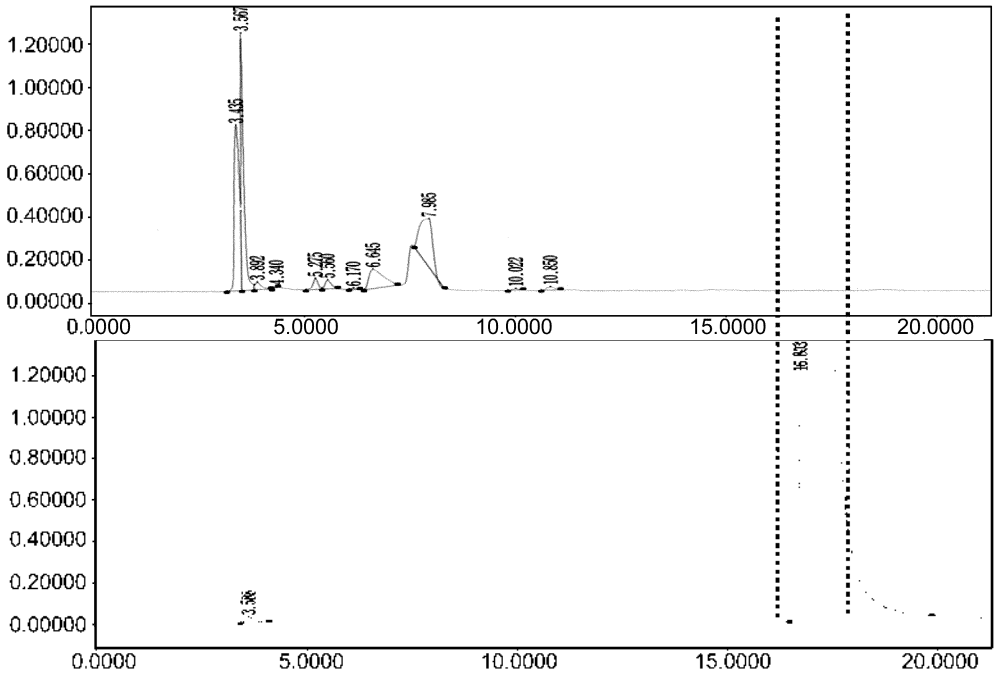

Figure 1. The radiochromatograms of [^{18}F]FPT reaction mixture. HPLC condition; column: LiChrosorb RP-18, 5 μ, 250 × 7.9 mm, mobile phase (ethanol:water:acetic acid = 10 : 87.5 : 2.5 [v/v/v] containing 2.5 g/L ammonium acetate), flow rate: 4 mL/min [upper: UV (267 nm), bottom: RI].

Table 1. Biodistribution Data of [^{18}F]FPT in Rats Bearing 9 L Tumor

Organ	Time point (min)			
	10	30	60	120
Blood	0.97 ± 0.62	0.63 ± 0.01	0.83 ± 0.23	0.52 ± 0.02
Liver	1.02 ± 0.11	0.72 ± 0.03	0.76 ± 0.10	0.60 ± 0.02
Lung	0.78 ± 0.08	0.57 ± 0.03	0.63 ± 0.07	0.50 ± 0.01
Spleen	1.10 ± 0.14	0.70 ± 0.05	0.68 ± 0.07	0.57 ± 0.03
Kidney	1.19 ± 0.19	0.83 ± 0.16	0.77 ± 0.09	0.58 ± 0.01
Stomach	0.50 ± 0.11	0.25 ± 0.02	0.29 ± 0.04	0.13 ± 0.01
Intestine	1.24 ± 0.20	0.70 ± 0.29	0.79 ± 0.23	0.57 ± 0.13
Femur	0.44 ± 0.06	0.49 ± 0.02	0.84 ± 0.09	0.92 ± 0.12
Thyroid	0.24 ± 0.07	0.14 ± 0.06	0.18 ± 0.10	0.15 ± 0.06
Tumor (9L)	0.71 ± 0.08	0.89 ± 0.29	1.24 ± 0.15	0.88 ± 0.26
Pancreas	2.46 ± 0.61	1.74 ± 0.17	1.42 ± 0.19	1.25 ± 0.19
Muscle	0.54 ± 0.05	0.54 ± 0.01	0.62 ± 0.07	0.45 ± 0.01
Brain	0.16 ± 0.01	0.20 ± 0.01	0.29 ± 0.03	0.26 ± 0.01

Number of mice/group; n = 3. Data represent as mean ± SD.

Table 2. Biodistribution Data of [^{18}F]FET in Rats Bearing 9L Tumor

Organ	Time point (min)			
	10	30	60	120
Blood	0.84 ± 0.07	0.69 ± 0.10	0.66 ± 0.03	0.69 ± 0.06
Liver	0.74 ± 0.06	0.64 ± 0.08	0.61 ± 0.02	0.62 ± 0.05
Lung	0.78 ± 0.05	0.66 ± 0.09	0.62 ± 0.01	0.61 ± 0.05
Spleen	0.93 ± 0.05	0.81 ± 0.12	0.73 ± 0.04	0.71 ± 0.04
Kidney	0.94 ± 0.12	1.08 ± 0.70	0.69 ± 0.10	0.64 ± 0.07
Stomach	0.45 ± 0.13	0.53 ± 0.20	0.42 ± 0.09	0.48 ± 0.09
Intestine	0.64 ± 0.09	0.58 ± 0.03	0.62 ± 0.08	0.57 ± 0.06
Femur	0.47 ± 0.03	0.45 ± 0.06	0.44 ± 0.01	0.45 ± 0.04
Thyroid	0.17 ± 0.01	0.13 ± 0.04	0.17 ± 0.05	0.19 ± 0.36
Tumor (9L)	0.68 ± 0.15	0.97 ± 0.13	1.19 ± 0.09	1.31 ± 0.54
Pancreas	2.58 ± 0.78	2.98 ± 0.24	3.01 ± 0.76	4.00 ± 0.54
Muscle	0.54 ± 0.06	0.62 ± 0.09	0.63 ± 0.01	0.63 ± 1.89
Brain	0.26 ± 0.02	0.35 ± 0.05	0.42 ± 0.02	0.54 ± 0.18

Number of mice/group; n=3. Data represent as mean ± SD.

clearance than [^{18}F]FET. The uptake of [^{18}F]FET in tumor, pancreas, and brain were increased as time-dependent manner, but the uptake of [^{18}F]FPT in tumor showed maximum values of 1.24 ± 0.15 at 60 min and it was decreased to 0.88 ± 0.26 at 120 min, and the uptake of [^{18}F]FPT in pancreas was decreased as a time-dependent manner. Biodistribution data of [^{18}F]FPT was similar to that of [^{18}F]FET, as previously reported.[14]

The ratios of tumor-to-blood (T/B), tumor-to-muscle (T/M) and tumor-to-brain (T/Br) for [^{18}F]FET and [^{18}F]FPT at 10, 30, 60 and 120 min postinjection are shown in Figure 2. T/B ratios of [^{18}F]FPT was similar with that of [^{18}F]FET and T/M ratios of [^{18}F]FPT was slight higher than that of [^{18}F]FET as time dependent manner, but T/Br ratios of [^{18}F]FPT was minimally 1.53 times higher than that of [^{18}F]FET at each time point. This result suggest that [^{18}F]FPT could be more useful than [^{18}F]FET for brain tumor imaging.

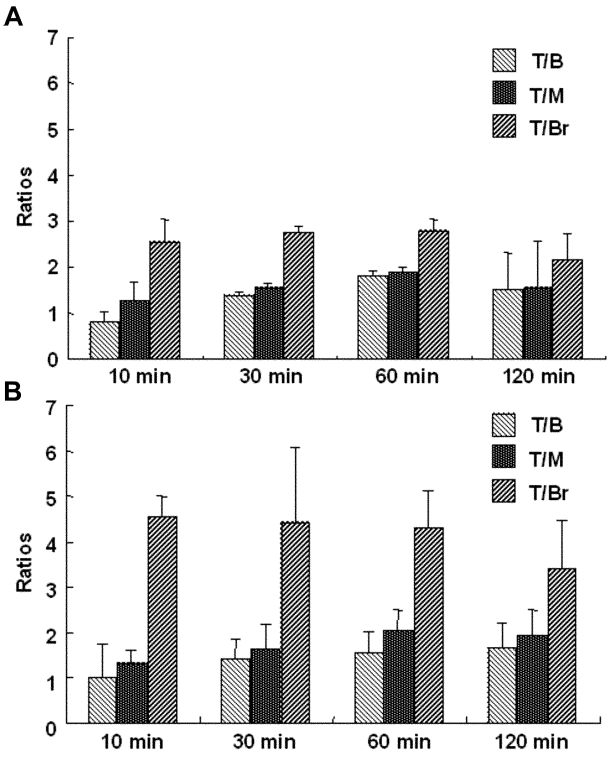

Figure 2. The ratios of tumor-to-blood (T/B), tumor-to-muscle (T/M) and tumor-to-brain (T/Br) of [^{18}F]FPT and [^{18}F]FET in rats bearing 9L tumor. (A) Ratios in [^{18}F]FET injected rats. (B) Ratios in [^{18}F]FPT injected rats at each time point. Data represent as mean ± S.D.

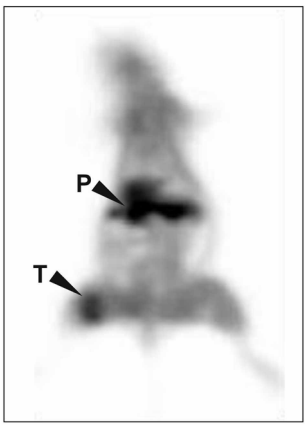

Figure 3. PET image of [^{18}F]FPT in 9L tumor bearing Fisher rat. [^{18}F]FPT was selectively localized in right thigh tumor of rat and also accumulated in pancreas. PET image was obtaned at 60 min postinjection. Tumor size was approximately about 1 cm.

[^{18}F]FET showed better correlation with [^{3}H]MET than [^{18}F]FTyr in the T/Br ratios in comparison study of [^{18}F]FET and [^{18}F]FTyr (2-[^{18}F]Fluoro-L-tyrosine) with [^{3}H]MET uptake in F98 rat gliomas.[18] In addition, our results demonstrated that [^{18}F]FPT showed better T/Br ratios than [^{18}F]FET in 9L tumor bearing rat. These results suggest that [^{18}F]FPT has a possibility to use a more useful brain tumor imaging agent than [^{18}F]FET.

PET Imaging. The coronal views of PET images of

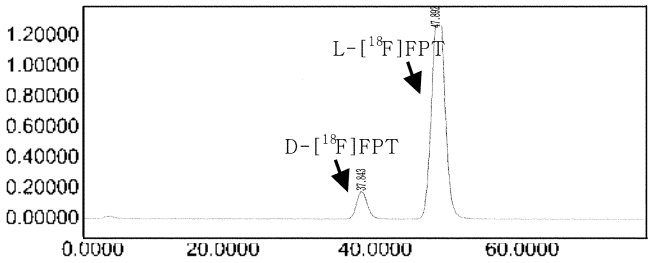

Figure 4. Chiral column (Crownpak CR (+), 150 × 4 mm, H_2O (pH = 2.0, $HClO_4$), flow rate: 0.8 mL/min)

tumor-bearing rats were obtained 60 min after administration of [^{18}F]FPT as shown in Figure 3. In PET images at 60 min, [^{18}F]FPT was selectively accumulated in 9L tumor of fisher 344 rat. [^{18}F]FPT also accumulated in pancreas. In recent reports, amino acid PET tracers showed pancreas uptake in rats and mice, which is in contrast to the observation of low [^{18}F]FET uptake in the pancreas of human. Such discrepancies in amino acid uptake in the pancreas between mice and humans have also been observed for [^{123}I]iodo-α-methyl-L-tyrosine, although the reasons for this difference remain unexplained.[5] These results suggest that [^{18}F]FPT could be used as amino acid tracer for the detection of brain tumor.

Partition Coefficient. The lipophilicity of [^{18}F]FPT (log P = −1.29) and [^{18}F]FET (log P = −1.43) were similar to previously reported result.[4]

Ratio of D- and L-[^{18}F]-FPT. The ratio of D-[^{18}F]-FPT and L-[^{18}F]-FPT was obtained by use chial column HPLC system as D-[^{18}F]-FPT: 37.8 min (7-9%), L-[^{18}F]-FPT 47.9 min (91-93%)) (n = 3).

Conclusion

[^{18}F]FPT was directly prepared from the precursor of *O*-(3-*p*-toluenesulfonyloxypropyl)-*N*-(*tert*-butoxycarbonyl)-L-tyrosine methyl ester, and the radiochemical yield and radiochemical purity were 40-45% and 95%, respectively. Biodistribution data of [^{18}F]FPT showed similar pattern with those of [^{18}F]FET, but [^{18}F]FPT showed higher tumor-to-brain ratio than [^{18}F]FET. Consequently, [^{18}F]FPT could be used as a new amino acid tracer for brain tumors imaging with PET.

Experimental Section

N-(*tert*-Butoxycarbonyl)-L-tyrosine methyl ester (97%), potassium carbonate (99.995%), (3-bromopropoxy)-*tert*-butyldimethylsilane (99%), tetrabutylammonium fluoride trihydrate, *p*-toluenesulfonyl chloride (99+%), triethylamine (TEA) (99+%), and 4,7,13,16,21,24-hexaoxa-1,10-diazabicyclo [8,8,8]hexacosane (Kryptofix®2.2.2.) (98%) were purchased from Aldrich Co. (U.S.A.) and Merck Co. (Germany). All solvents were of either analytical or HPLC grade and used without further purification. Thin layer chromatography (TLC) was performed on Merck 60 F_{254} silica plates and visualized by UV. Flash column chromatography was performed on silica gel 230-400 mesh. High Performance Liquid Chromatography (HPLC) was carried out on a Young-Lin System (Young-Lin Instrument, Korea) with a semi preparative column (Lichrosorb® RP-18, 5 μ, 7.9 × 250 mm from Merck, Germany) and simultaneously monitored by a Young-Lin UV instrument (267 nm) and Raytest GABI γ-detector. F-18 was produced with MC-50 cyclotron by irradiation of $H_2{}^{18}O$ at Korea Institute of Radiological and Medical Sciences (KIRAMS). Radio-TLC was measured on a Bioscan AC-3000 scanner (Washington D.C., U.S.A.). All radiochemical yields are decay-corrected unless noted. ^{1}H- and ^{13}C-NMR spectra were recorded on a Bruker-300 and chemical shifts were reported in δ units (ppm) from internal standard tetramethylsilane. Mass spectra were obtained on a JMS700 spectrometer (JEOL Co., Japan).

***O*-(3-*tert*-Butyldimethylsilyloxypropyl)-*N*-(*tert*-butoxycarbonyl)-L-tyrosine Methyl Ester (2).** *N*-(*tert*-Butoxycarbonyl)-L-tyrosine methyl ester (790 mg, 2.67 mmol) was dissolved in 10 mL of DMF. To the stirred mixture, potassium carbonate (406 mg, 2.94 mmol) and 3-(bromopropoxy)-*tert*-butyldimethylsilane (678 μL, 2.94 mmol) were added and stirred for 3 days under a stream of N_2 at room temperature. The DMF was removed under reduced pressure. The residue was extracted with ethyl acetate and washed by water and then crude product was obtained. Flash column chromatography (20% EtOAc/hexane) gave colorless oil **2** (467 mg, 42%): ^{1}H NMR (300 MHz, $CDCl_3$) δ 7.01 (d, 2H, J = 8.7 Hz), 6.81 (d, 2H, J = 8.7 Hz), 4.93-4.96 (m, 1H), 4.52-4.54 (m, 1H), 4.03 (t, 2H, J = 6.3 Hz), 3.79 (t, 2H, J = 6.3 Hz), 3.70 (s, 3H), 3.00-3.03 (m, 2H), 1.96 (p, 2H), 1.42 (s, 9H), 0.88 (s, 9H), 0.04 (s, 6H); ^{13}C NMR (75 MHz, $CDCl_3$) δ 172.5, 158.2, 155.1, 130.2, 127.7, 114.6, 79.9, 64.5, 59.5, 54.6, 52.2, 37.5, 32.4, 28.3, 25.9, 18.3, -5.4; MS (FAB) m/z: 468 (MH^+); HRMS (FAB) calcd for $C_{24}H_{42}NO_6Si$ ($M+Na^+$) 490.2613, found 490.2607.

***O*-(3-Hydroxypropoxy)-*N*-(*tert*-butoxycarbonyl)-L-tyrosine Methyl Ester (3).** To a round bottom flask, *O*-(3-*tert*-butyldimethylsilyloxypropyl)-*N*-(*tert*-butoxycarbonyl)-L-tyrosine methyl ester (1.47 g, 3.14 mmol) and 10 mL of tetrahydrofuran was added. After TBAF·3H_2O (1.08 g, 3.45 mmol) were added and stirred for 5 min at room temperature. The reaction mixture was concentrated in vacuo. Flash column chromatography (40% EtOAc/hexane) gave colorless oil **3** (776 mg, 70%): ^{1}H NMR (300 MHz, $CDCl_3$) δ8.07 (s, 1H), 7.03 (d, 2H, J = 8.7 Hz), 6.83 (d, 2H, J = 8.7 Hz), 4.95-4.98 (m, 1H), 4.53-4.55 (m, 1H), 4.37 (t, 2H, J = 6.3 Hz), 3.79 (t, 2H, J = 6.3 Hz), 3.71 (s, 3H), 3.00-3.04 (m, 2H), 2.16 (p, 2H), 1.42 (s, 9H); ^{13}C NMR (75 MHz, $CDCl_3$) δ 172.4, 161.0, 157.8, 130.3, 128.2, 114.5, 80.0, 64.0, 60.8, 54.5, 52.2, 37.5, 29.7, 28.3; MS (FAB) m/z: 376 ($M+Na^+$); HRMS (FAB) calcd for $C_{18}H_{27}NO_6$ ($M+Na^+$) 376.1736, found 376.1753.

***O*-(3-*p*-Toluenesulfonyloxypropyl)-*N*-(*tert*-butoxycarbonyl)-L-tyrosine Methyl Ester (4).** *O*-(3-Hydroxypropyl)-*N*-(*tert*-butoxycarbonyl)-L-tyrosine methyl ester (1.20 g, 3.39 mmol) was dissolved in 10 mL of anhydrous

dichloromethane. To a stirred mixture, *p*-toluenesulfonyl chloride (969 mg, 5.09 mmol) and TEA (944 μL, 6.78 mmol) were added and stirred for 3 h at room temperature. The reaction mixture was concentrated in vacuo. Flash column chromatography (30% EtOAc/hexane) gave colorless oil **4** (1.37 g, 80%): ^{1}H NMR (300 MHz, $CDCl_3$) δ 7.76 (d, 2H, J = 8.1 Hz), 7.26 (d, 2H, J = 8.1 Hz), 7.01 (d, 2H, J = 8.7 Hz), 6.70 (d, 2H, J = 8.7 Hz), 4.96-4.98 (m, 1H), 4.53-4.55 (m, 1H), 4.24 (t, 2H, J = 6.0 Hz), 3.93 (t, 2H, J = 6.0 Hz), 3.72 (s, 3H), 3.00-3.05 (m, 2H), 2.41 (s, 3H), 2.09 (p, 2H), 1.42 (s, 9H); ^{13}C NMR (75 MHz, $CDCl_3$) δ 172.4, 155.2, 144.7, 132.9, 130.2, 129.8, 128.3, 127.9, 114.5, 79.9, 67.1, 63.1, 54.6, 52.2, 37.5, 28.9, 28.3, 21.6; MS (FAB) m/z: 508 (MH^+); HRMS (FAB) calcd for $C_{25}H_{34}NO_8S$ (MH^+) 508.2005, found 508.2001.

***O*-(3-Fluoropropyl)-L-tyrosine (FPT) (5).** *O*-(3-*p*-Toluenesulfonyloxypropyl)-*N*-(*tert*-butoxycarbonyl)-L-tyrosine methyl ester (208 mg, 0.41 mmol) and TBAF·3H_2O (258.7 mg, 0.82 mmol) were dissolved in anhydrous acetonitrile and stirred for 20 min at 90 °C. The solvents was removed under reduced pressure followed by the residue was poured into 10 mL of water and extracted with ethyl acetate. The extracted solution was dried over anhydrous Na_2SO_4, filtered and evaporated under reduced pressure. Flash column chromatography (25% EtOAc/hexane) gave *O*-(3-fluoropropyl)-*N*-(*tert*-butoxycarbonyl)-L-tyrosine methyl ester (123 mg, 51%). The fluorinated tyrosine derivative was added in acetonitrille and dissolved then 4 N HCl (2 mL) was added and stirring continued for 40 min at 110 °C. The organic solvents were removed under reduced pressure and poured into a little water. When pH value was regulated in 7.5 white color precipitate was produced in the aqueous solution which was filtered and washed with water and dried. The crude product was recrystallized from 60% acetic acid to give a white crystal of FPT **5** (88 mg, 44%): mp: 234-237 °C; ^{1}H NMR (300 MHz, DMSO-d_6) δ 13.74 (brs, 1H), 8.44 (brs, 2H), 7.20 (d, 2H, J = 9.0 Hz), 6.91 (d, 2H, J = 9.0 Hz), 4.60 (dt, 2H, J = 47.4, 5.8 Hz), 4.03-4.10 (m, 3H), 3.08 (d, 2H, J = 6.0 Hz), 2.08 (dq, 2H, J = 26.8, 8.4 Hz); ^{13}C NMR (75 MHz, DMSO-d_6) δ 170.7, 158.1, 131.1, 127.4, 115.0, 81.3 (d, J = 165.0 Hz), 64.0 (d, J = 7.5 Hz), 53.8, 35.3, 30.3 (d, J = 22.5 Hz); MS (FAB) m/z: 242 (MH^+); HRMS (FAB) calcd for $C_{12}H_{17}NO_3F$ (MH^+) 242.1192, found 242.1190.

Preparation and Purity of *O*-(3-[^{18}F]Fluoropropyl)-L-tyrosine ([^{18}F]FPT). To a reaction vial containing 1 mL of dry acetonitrile, aqueous [^{18}F]fluoride solution (37 GBq) was added, followed by 5-7 mg of Kryptofix®2.2.2 and 150 μL of potassium carbonate solution (0.03 M) were added. The solvent was removed by the stream of nitrogen gas at 80 °C. Azeotropic drying was repeated at least three times with 0.5 mL of acetonitrile. To a reaction vial, 8-10 mg of *O*-(3-*p*-toluenesulfonyloxypropyl)-*N*-(*tert*-butoxycarbonyl)-L-tyrosine methyl ester was added and dissolved in 1.0 mL of acetonitrile. The reaction mixture was stirred for 25 min at 90 °C and the reaction was monitored by radio-TLC. After completion, HCl (4 N, 1.5 mL) was added and the mixture was hydrolyzed for 40 min at 110 °C under open system. The reaction mixture was purified by HPLC using a semi-preparative column. The further purification was done by loading the purified [^{18}F]FPT through the strong cation exchange resin and collected pure [^{18}F]FPT with the phosphate buffered solution (9 mL, pH = 7.4) and sodium bicarbonate solution (2.5 mL, 8.4%) mixture. After final formulation was achieved by sterile filtration with Millex-GV (0.22 micron filter). Quality control was performed by HPLC (LiChrosorb RP-18, 250 × 4 mm, chiral column (Crownpak CR (+), 150 × 4.0 mm)) and thin-layer chromatography (SiO_2, water : acetonitrile = 2 : 8 [v/v]). Radiochemical yields is about 40-45% and radiochemical purity was more than 95%. The specific activity after HPLC purification was > 37 GBq/μmol.

Tumor Model. The study was performed according to the guidelines of the Korea Institute of Radiological and Medical Sciences. Female and male Fisher 344 rats, weighing 130-150 g, were purchased from the Charles River Laboratories (Wilimington, MA, USA) and were used to prepare tumor-bearing model. All the animals were kept in cages with standardized conditions of light, asepsis and free access to water and food. Mice were inoculated with 9L glioma cell in the right thigh of rats. Experiments were perfonned 7-14 days after inoculation of the tumor cells. At this time, the tumors weighed 1.9-3.3 g and a tumor diameter of more than 1.0-2.5 cm cm was observed.

Biodistribution Studies. The animals were anesthetized with ethylether before injection of radiotracer and remained anesthetized through the study. Mice were injected with 370 MBq (1.0 Ci) of [^{18}F]FPT and [^{18}F]FET in 100-200 μL of saline through the tail vein, respectively. After each tracer injection, biodistribution was performed at 10, 30, 60, and 120 min. Blood was obtained through cardiac puncture, and the tissue samples of interest, including blood, brain, lung, liver, kidney, spleen, intestine, muscle, femur, and pancreas in 9L tumor bearing rats. All samples were weighed, and the radioactivity was measured using NaI crystal well-type gamma counter (Wallac Wizard Co, USA), applying a decay correction. Counts were compared with those of standards, and the results were expressed as percentage of injected radioactivity dose per gram of tissue (%ID/g).

PET Studies. After 60 min of intravenous injection of each PET tracer (each 37 MBq), rats were sacrificed with lethal dose of ethylether. Using dedicated PET scanner (ECAT EXACT HR+ scanner, SIEMENS/CTIMI, Knoxville, Tenn), acquisition was performed in 2-dimensional mode. Using a germanium-68 source, transmission images were obtained for 5 min to correct for photon attenuation. After the transmission scan, emission images were obtained for 15 min, and acquisition data were reconstructed using iterative reconstruction and segmented attenuation. The total acquisition time was 20 min.

Measurement of Partition Coefficient. The partition coefficient of [^{18}F]FPT was measured using 2.0 mL of 1-octanol as the organic phase and 2.0 mL 0.15 mol/L phosphate buffer (pH 7.4) as the aqueous phase. Ten

microliters of the radioactive sample in PBS buffer were added and mixed for 2 min at room temperature. The radioactivity of 500 μL of each phase was measured.

Separation of D-[^{18}F]FPT and L-[^{18}F]FPT. D-[^{18}F]FPT and L-[^{18}F]FPT ratio were checked using by chiral column (Crownpak CR (+), 150 × 4.0 mm).

Synthesis of L-[^{18}F]FET. L-[^{18}F]FET was synthesized as published previously by Tang *et al.*[15]

Acknowledgement. This work was supported by Nuclear R&D Program from the Ministry of Science & Technology.

References

1. Rigo, P.; Paulus, P.; Kaschten, B. J.; Hustinx, R.; Bury, T.; Jerusalem, G.; Benoit, T.; Foidart-Willems, J. *Eur. J. Nucl. Med.* **1996**, *23*, 1641-1674.
2. Shreve, P. D.; Anzai, Y.; Wahl, R. L. *Radiographics* **1999**, *19*, 61-77.
3. Weber, W. A.; Wester, H. J.; Grosu, A. L.; Herz, M.; Dzewas, B.; Feldmann, H. J.; Molls, M.; Stocklin, G.; Schwaiger, M. *Eur. J. Nucl. Med.* **2000**, *27*, 542-549.
4. Wester, H. J.; Herz, M.; Weber, W.; Heiss, P.; Senekowitsch-Schmidtke, R.; Schwaiger, M.; Stocklin, G. *J. Nucl. Med.* **1999**, *40*, 205-212.
5. Heiss, P.; Mayer, S.; Herz, M.; Wester, H. J.; Schwaiger, M.; Senekowitsch-Schmidtke, R. *J. Nucl. Med.* **1999**, *40*, 1367-1373.
6. Shoup, T. M.; Olson, J.; Hoffman, J. M.; Votaw, J.; Eshima, D.; Eshima, L.; Camp, V. M.; Stabin, M.; Votaw, D.; Goodman, M. M. *J. Nucl. Med.* **1999**, *40*, 331-338.
7. Wester, H. J.; Herz, M.; Senekowitsch-Schmidtke, R.; Schwaiger, M.; Stocklin, G.; Hamacher, K. *Nucl. Med. Biol.* **1999**, *26*, 259-265.
8. Kubota, K.; Ishiwata, K.; Kubota, R.; Yamada, S.; Takahashi, J.; Abe, Y.; Fukuda, H.; Ido, T. *J. Nucl. Med.* **1996**, *37*, 320-325.
9. Hustins, R.; Lemaire, C.; Jerusalem, G.; Moreau, P.; Cataldo, D.; Duysinx, B.; Aerts, J.; Fassotte, M. F.; Foidart, J.; Luxen, A. *J. Nucl. Med.* **2003**, *44*, 533-539.
10. Shikano, N.; Kawai, D.; Flores, L. G.; Nishii, R.; Kubota, N.; Ishikawa, N.; Kubodera, A. *J. Nucl. Med.* **2003**, *44*, 625-631.
11. Inoue, T.; Tomiyoshi, K.; Higuichi, T.; Ahmed, K.; Sarwar, M.; Aoyagi, K.; Amano, S.; Alyafei, S.; Zhang, H.; Endo, K. *J. Nucl. Med.* **1998**, *39*, 663-667.
12. Langen, K. J.; Muhlensiepen, H.; Holschbach, M.; Hautzel, H.; Jansen, P.; Coenen, H. H. *J. Nucl. Med.* **2000**, *41*, 1250-1255.
13. Chen, J. C.; Chang, S. M.; Hsu, F. Y.; Wang, H. E.; Liu, R. S. *Appl. Radiat. Isot.* **2004**, *61*, 887-891.
14. Tang, G.; Wang, M.; Tang, X.; Luo, L.; Gan, M. *Nucl. Med. Biol.* **2003**, *30*, 733-739.
15. Tang, G.; Tang, X.; Wang, M.; Luo, L.; Gan, M. *Appl. Radiat. Isot.* **2003**, *58*, 685-689.
16. Tang, G.; Tang, X.; Wang, M.; Luo, L.; Gan, M. *Appl. Radiat. Isot.* **2004**, *60*, 27-32.
17. Lee, K. C.; Lee, S. Y.; Choe, Y. S.; Chi, D. Y. *Bull. Korean Chem. Soc.* **2004**, *25*, 1225-1230.
18. Langen, K. J.; Jarosch, M.; Muhlensiepen, H.; Hamacher, K.; Broer, S.; Jansen, P.; Zilles, K.; Coenen, H. H. *Nucl. Med. Biol.* **2003**, *30*, 501-508.